

MINISTRY OF INDUSTRY AND TRADE

**HANOI UNIVERSITY OF INDUSTRY**

-----



**NGUYEN DUY TRINH**

**STUDY ON IMPROVING SURFACE QUALITY WHEN  
MAGNETORHEOLOGICAL POLISHING TI-6AL-4V ALLOY**

Major: Mechanical Engineering

Code: 9.52.01.03

**SUMMARY OF DESERTATION IN ENGINEERING**

**Hanoi, 2025**

This desertation has been completed at:

**HANOI UNIVERSITY OF INDUSRY**

**Scientific supervisors:**

**Assoc. Prof. Dr. Hoang Tien Dung**

*Reviewer 1:*

*Reviewer 2:*

*Reviewer 3:*

The desertation was defended at the Doctoral Evaluating Council at University level, held at Hanoi University of Industry at ....., date..... 20.....

**The thesis can be accessed at:**

- Library of Hanoi University of Industry
- National Library of Vietnam

## INTRODUCTION

### 1. Rationale for the thesis topic

Ti-6Al-4V alloy is widely used in many industries, including aerospace, sports equipment, petrochemical, medical and automotive, among other high-tech industries. The wide application of this material is promoted by the combination of outstanding advantages such as light weight (only 56% compared to stainless steel), high biocompatibility, along with excellent corrosion resistance and high strength [1-3]. With its outstanding fatigue strength and high heat resistance, this allows titanium and its alloys to be used in important applications such as gas turbines in the aerospace industry, with the ability to withstand temperatures up to 600°C [4, 5]. In the working conditions of structures subjected to cyclic rotational loads and high temperatures in the aviation industry such as jet engine main shafts, turbine rotors, engine fan shafts, high-pressure compressor shafts, helicopter main rotor shafts and landing gear shafts, fatigue cracks often originate from small scratches formed during machining. Scratches formed during machining are one of the main causes of fatigue crack initiation and propagation, leading to damage to the working surface of machine parts. Therefore, studying solutions to reduce scratches on the surface of parts manufactured from Ti-6Al-4V alloy helps limit the development of fatigue cracks [6, 7]. In addition, when using Ti-6Al-4V alloy in the production of micro-electromechanical systems (MEMS), increased surface roughness can lead to lower fatigue life, increased mechanical wear and a higher risk of surface cracking. On the contrary, when the surface roughness is low, the durability and performance of these devices are significantly improved.

The demand for equipment using Ti-6Al-4V material parts with nanometer roughness and large area has increased rapidly in many fields, such as aerospace, petrochemical industry and medicine [8, 9]. MRF polishing methods respond well and produce mirror-like surfaces with nanometer roughness. With two common types of magnetic polishing used including ball head and grinding wheel [10-12], which are used to polish large surfaces along the tool trajectory. These models have low polishing efficiency and require long processing time. Therefore, when applied in industrial production and especially large-sized surfaces, a lot of polishing time is needed. The performance and efficiency of magnetic polishing can be improved by increasing the magnetic field strength and expanding the working area of the magnetic polishing machine. Wang et al. [13] proposed a permanent magnetic yoke to produce super-smooth surfaces; In this study, a wide magnetic field was achieved and demonstrated to be effective in MRF polishing processes with large surfaces. An improved magnetic yoke was developed by Luo et al. [14] to produce large-sized medical ceramic (zirconia) surfaces with efficient material removal and high surface quality.

However, with the developed magnetic yokes, the magnetic field in the polished area does not extend infinitely due to the limitations of the magnetic yoke size as well as the magnetic field generation capability. An infinite magnetic field array generated through the arrangement of magnets can overcome the limitations encountered in the magnetic field generation process. Meng et al. [15] developed a polishing process using magnet clusters in MRF polishing processes to expand the magnetic field operating capability. The magnetic field density distribution and polishing performance were verified through experiments and simulations. However, research has focused on generating magnetic fields through simple magnet arrangement methods and has not explored methods to improve surface quality and remove residual machining material in MRF polishing processes by increasing the magnetic field strength. An ideal solution that can improve the polishing efficiency of MRF is to increase the magnetic field strength using Halbach arrays [16, 17]. Halbach magnetic arrays enhance the magnetic field strength and expand the excitation zone, thereby increasing the polishing efficiency in MRF processes. In particle accelerators, high-performance motors, magnetic resonance imaging, and magnetic analyzers, Halbach arrays are often used to generate high-intensity magnetic fields concentrated on one side while using several small magnets [18, 19]. Furthermore, Halbach arrays easily expand the magnetic field generation zone, thus contributing to the polishing efficiency of large-plane magnetic liquid solutions.

Based on the challenges in precision machining of Ti-6Al-4V alloy and the above analysis, the researcher proposed a new approach through the topic: **“STUDY ON IMPROVING SURFACE QUALITY WHEN MAGNETORHEOLOGICAL POLISHING TI-6AL-4V ALLOY”**. With the new approach based on combining MRF polishing technology with an optimized Halbach magnetic array configuration to increase the magnetic field strength and expand the polishing area, thereby improving material removal efficiency while maintaining precision and surface roughness at the nanometer level. Another important improvement is established through the new MRF solution using environmentally friendly ingredients such as  $\text{Fe}_3\text{O}_4$ ,  $\text{SiO}_2$ ,  $\text{H}_2\text{O}_2$ , malic acid and purified water. The magnetic solution system is established to ensure effective polishing, while minimizing the impact on health and the environment, in line with green manufacturing orientation.

## **2. Research objectives**

### ***General Objective:***

Research and develop a detailed magnetic polishing (MRF) process for Ti-6Al-4V alloy material to achieve nanometer surface roughness.

### ***Specific Objectives:***

- Design an MRF polishing device using an improved Halbach array to increase the intensity and expand the magnetic field impact area.
- Analyze the selection of MRF polishing solutions using  $\text{Fe}_3\text{O}_4$  magnetic particles,  $\text{SiO}_2$  abrasive particles,  $\text{H}_2\text{O}_2$  oxidant and malic acid to ensure high performance while still being environmentally safe.
- Verify the mathematical model of cutting force through experimental analysis. Integrate the Preston equation with FT and FN force components in the mathematical model to improve the accuracy of predicting material removal rate (MRR).

### **3. Research scope and objects**

#### **3.1. Research objects**

- The improved Halbach array is designed to generate a strong magnetic field and a large area of effect in the MRF magnetic polishing zone of Ti-6Al-4V alloy parts.
- The environmentally friendly MRF magnetic polishing solution is designed based on  $\text{Fe}_3\text{O}_4$  magnetic particles,  $\text{SiO}_2$  abrasive particles,  $\text{H}_2\text{O}_2$  oxidant, purified water and malic acid, to improve the material removal ability and achieve nanometer-level surface roughness.

#### **3.2. Research scope**

Study on surface quality and material removal ability of magnetic polishing (MRF) process for Ti-6Al-4V alloy using environmentally friendly MRF solution including:  $\text{Fe}_3\text{O}_4$  magnetic particles,  $\text{SiO}_2$  abrasive particles,  $\text{H}_2\text{O}_2$  oxidant and malic acid, combined with improved Halbach array. Research parameters include:

- Technological parameters: rotation speed of the workpiece ( $200 \div 600$  rpm), polishing distance ( $1.0 \div 2.0$  mm), number of reciprocating cycles of Halbach array ( $15 \div 30$  cycles/min), MRF solution volume ( $300 \div 600$  ml).
- MRF solution parameters:  $\text{H}_2\text{O}_2$  concentration ( $0.5 \div 1.5\%$  by volume), pH value of the solution ( $4 \div 6$ ).

### **4. Research contents**

*To achieve the stated research objectives, the thesis focuses on carrying out the following main contents:*

- Overview of magnetic polishing technology, focusing on the application of MRF for Ti-6Al-4V alloy. The content includes a synthesis and analysis of domestic and foreign research on MRF, an assessment of the development progress, operating mechanism and practical application. In particular, the study focuses on establishing MRF solution using  $\text{Fe}_3\text{O}_4$ ,  $\text{SiO}_2$  and  $\text{H}_2\text{O}_2$  to improve polishing performance, and identifies key research issues that need to be addressed to optimize the polishing process of Ti-6Al-4V alloy.
- Study the principle of MRF magnetic polishing and the magnetic field and polishing force settings in machining Ti-6Al-4V

alloy. Based on a detailed analysis of the material removal mechanism and apparent viscosity, an improved Halbach magnetic array is established to enhance the magnetic field generation and polishing force. The content of this chapter focuses on evaluating the factors affecting the magnetic force acting on the magnetic particle, and at the same time building a mathematical model of the polishing force when using the reciprocating Halbach array.

- The experiments are built on the basis of single-factor analysis to determine the appropriate parameter range for the MRF polishing process. Ti-6Al-4V alloy is polished with a solution containing  $\text{Fe}_3\text{O}_4$ ,  $\text{SiO}_2$ , malic acid and  $\text{H}_2\text{O}_2$ , in which the influence of  $\text{H}_2\text{O}_2$  concentration and pH on the polishing performance is studied in detail.

- Conduct experiments and optimize some MRF polishing technology parameters. First, the study verifies the cutting force model and material removal in the MRF polishing process with the reciprocating Halbach array. Next, orthogonal experiments were used to simultaneously analyze important process parameters such as polishing distance, slurry volume, workpiece rotation speed, and Halbach plate double stroke number. The obtained data were processed using range analysis to determine the optimal process parameters, aiming at achieving low surface roughness and high material removal.

## 5. Research methods

The thesis uses theoretical research methods combined with experiments and technology applications with the following main contents:

- **Theoretical research:** Analyze and evaluate technological factors affecting the magnetic polishing process, including magnetic field strength, workpiece rotation speed, Halbach array moving speed, polishing distance and MRF solution volume.

- **Simulation research:** Apply COMSOL Multiphysics software to simulate the magnetic field to determine the improved Halbach array arrangement method, creating a strong magnetic force with a high gradient concentrated on one side, thereby optimizing the design and improving the efficiency of MRF magnetic polishing.

- **Experimental research:** MRF polishing experiments on Ti-6Al-4V alloy were established to verify the constructed mathematical models. The experiments were conducted with changing technological factors such as  $\text{H}_2\text{O}_2$  concentration, pH of the solution, polishing distance and Halbach array moving speed. Using data processing methods to analyze experimental results, evaluate the relationship between technological factors and surface quality as well as material removal capacity.

## 6. Scientific and practical significance

### **6.1. Scientific significance**

Establishing an improved Halbach magnetic polishing model with an environmentally friendly magnetic solution. Applying the model to improve productivity and surface roughness when polishing Ti-6Al-4V alloy materials.

Building and verifying a mathematical model describing the tangential force ( $F_T$ ) and normal force ( $F_N$ ) in the magnetic polishing process, creating a theoretical basis for determining the material removal ability and improving the surface quality of Ti-6Al-4V materials. Through magnetic field simulation and experimental design, the study elucidates the mechanism of removing excess machining material and analyzes the main factors affecting the surface quality, thereby opening up high application potential in polishing Ti-6Al-4V alloy.

### **6.2. Practical significance**

The results of the study provide a basis for selecting technical parameters in the magnetic polishing process of titanium alloys, and serve as a reference in supporting research, training and development of magnetic machining and polishing techniques. This study lays the foundation for the application of advanced and flexible polishing technology in production to improve surface quality in high-precision industries.

## **7. Innovations of the thesis**

An improved Halbach array with a strong magnetic field and high gradient is proposed to increase the polishing force and thereby enhance the material removal ability, which improves the polishing efficiency of Ti-6Al-4V alloy MRF.

The MRF polishing process uses an environmentally friendly solution consisting of  $\text{SiO}_2$ ,  $\text{Fe}_3\text{O}_4$  abrasives,  $\text{H}_2\text{O}_2$  oxidants and malic acid, which achieves high removal efficiency of machined material residue with nanometer surface roughness and is environmentally safe, in line with the trend of sustainable manufacturing.

The mathematical model describing the tangential and normal forces achieves high accuracy (error <16%), allowing prediction of machined material residue removal efficiency and optimization of surface roughness, opening up wide application potential in high-precision industries such as aerospace, medical and petrochemical.

## **8. Structure of the disseration.**

The dissertation is structured beyond the parts: Introduction, Conclusion, and Further Research Directions, with the research content presented in 4 chapters:

Chapter 1. Overview of magnetic polishing methods.

Chapter 2. Building a magnetic polishing model using improved Halbach array.

Chapter 3. Experimental design of magnetic polishing using improved Halbach array to process Ti-6Al-4V alloy.

Chapter 4. Results and analysis.

## **CHAPTER 1**

### **OVERVIEW OF MAGNETORHEOLOGICAL FINISHING METHODS**

Chapter 1 focuses on research related to:

- Research situation at home and abroad.
- Magnetic polishing technology.
- Some methods of magnetic polishing of Titanium alloys.
- Challenges when magnetic polishing of Titanium alloys.
- Analysis of magnetic solution when polishing Ti-6Al-4V alloy material.

Subsequently, several conclusions are drawn as follows:

1. Titanium alloys are widely used due to their light weight, high strength, heat resistance and corrosion resistance, but the surface finishing process is challenging.
2. Magnetorheological finishing (MRF) technology helps to precisely control the polishing force by magnetorheological fluid, allowing to achieve nanometer surface roughness, suitable for high requirements in biomedicine and aerospace.
3. Comparative study of MRF performance with other methods such as MFAF, MRAFF, R-MRAFF, in which disc-shaped MRF is highly appreciated for machining flat surfaces.
4. Proposing the use of Halbach magnetic array combined with MRF solution containing  $\text{SiO}_2$ ,  $\text{Fe}_3\text{O}_4$ ,  $\text{H}_2\text{O}_2$  and malic acid, to improve polishing performance and ensure environmental friendliness.

## **CHAPTER 2**

### **DEVELOPMENT OF A MAGNETORHEOLOGICAL POLISHING MODEL USING IMPROVED HALBACH ARRAY**

#### **2.1. Principle and apparent viscosity in magnetic polishing**

The magnetic polishing process is based on the effect of a magnetic field on the MRF solution, creating a cutting force on the machined surface. When subjected to the magnetic field, the magnetic particles in the MRF are linked into chains, increasing the apparent viscosity and changing the state of the solution from liquid to semi-solid. The polishing mechanism is similar to the cutting process, in which the material surface undergoes elastic and plastic



deformation and is microscopically removed. Apparent viscosity plays an important role in the material removal ability, helping to control the cutting force and achieve super-smooth surface roughness.

## 2.2. Establishing the magnetic polishing scheme with the improved Halbach array

### 2.2.1. Determining the optimal Halbach array through the recovery function

The optimal Halbach array with magnet sizes of 30 mm in height and 25 mm in width is used in the analysis, thereby showing the superiority of the proposed Halbach over the conventional magnet arrays. The conventional interleaved magnets have width and height dimensions of 40 mm. The recovery is determined as a function of the magnetic moment with the analysis results in Fig. 2.1. In which three different Halbach configurations with sequential arrangement methods are investigated through the recovery ability.

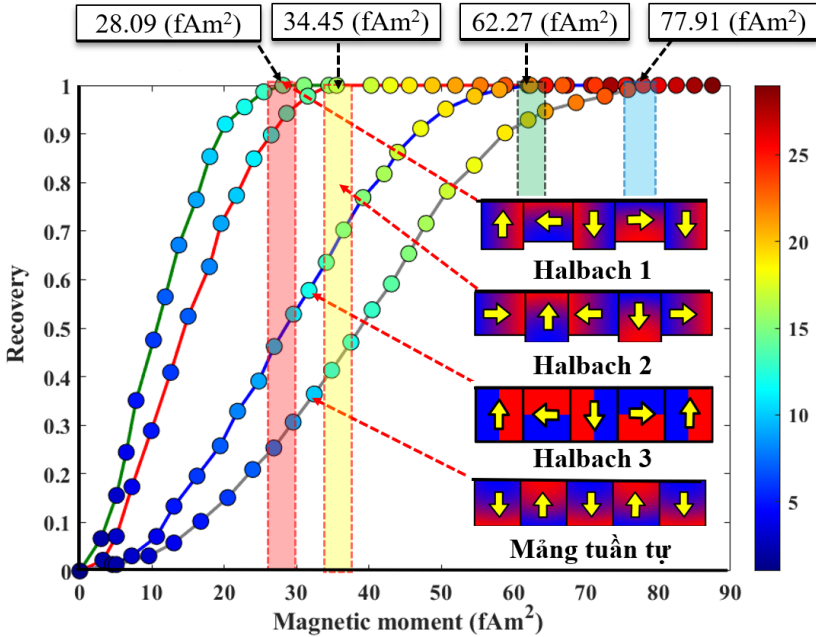


**Fig. 2.1** MRF ribbon recovery capability under different magnet array arrangement methods

The analysis results show that Halbach 1 and Halbach 2 arrays with dimensions of  $30 \times 25$  mm and  $25 \times 30$  mm, respectively. Halbach 3 arrays and conventional arrays of  $30 \times 30$  mm and  $40 \times 40$  mm have magnetic moments of 28.09, 34.45, 62.27 and 77.91 ( $\text{fAm}^2$ ) respectively for 100% recovery. This analysis highlights the contributions of the proposed Halbach arrays, especially

the  $30 \times 25$  mm magnet array used, to the optimal recovery performance. Notably, when Halbach 1 array achieved 100% recovery with a magnetic moment of  $28.09$  (fAm<sup>2</sup>), which is lower than the other arrays, it shows that Halbach 1 array is a good choice for high efficiency with MRF polishing process.

### 2.2.2. Magnetic force acting on magnetic particles in the presence of a magnetic field

Simulation using COMSOL Multiphysics software shows the distribution of magnetic field gradients and magnetic fluxes corresponding to different magnet structures (Fig. 2.2). The results show that as the magnetic field gradient increases, the magnetic field parameters decrease. When the magnets are arranged perpendicular to each other, the magnetic field lines are strongly concentrated on one side, creating an asymmetric magnetic field structure. Magnet arrays arranged in this configuration are called Halbach arrays. In which, Halbach 1 and Halbach 2 arrays create a magnetic field more concentrated on one side than Halbach 3 array (conventional Halbach array) and compared to the sequential arrangement of magnets using the conventional method.

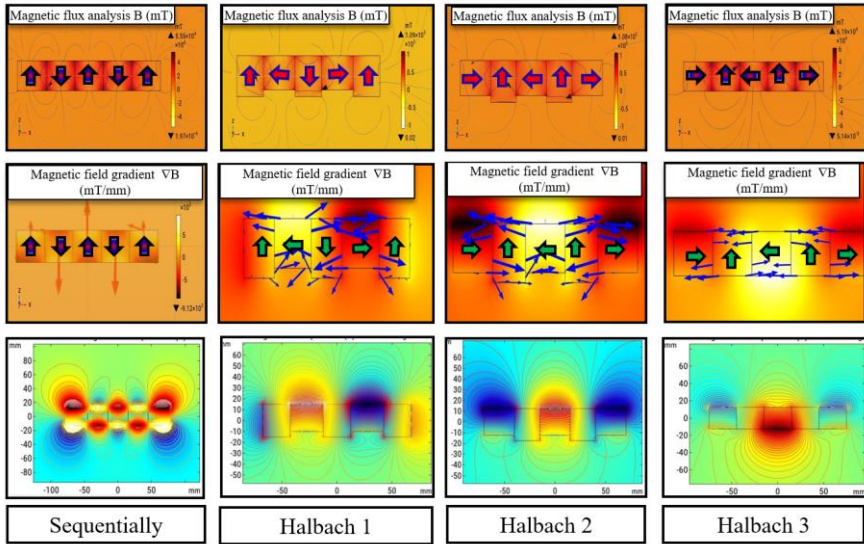


**Fig. 2.2** Magnetic field gradients and strengths obtained through different magnet arrangement methods

### 2.2.3. Repulsive and attractive forces acting on magnetic particles

In MRF polishing processes, the flow of liquid around magnetic particles creates a resistance force. When subjected to a magnetic field, spherical Fe<sub>3</sub>O<sub>4</sub>

particles experience a resistance force, which is determined by factors such as particle velocity, particle radius  $R$ , viscosity  $\eta$ , and velocity of the magnetic fluid flow [20]. This resistance force is calculated based on the following equation:

$$F_T = 6\eta\pi R(v_p - v_f) \quad (2.10)$$

The magnetic particles in the MRF solution with the gravitational force in the carrier solution create is called the attractive force, described by the following equation:

$$F_G = V_p \times g \times (\rho_p - \rho_f) \quad (2.11)$$

### 2.3. Application of improved Halbach array in magnetorheological polishing

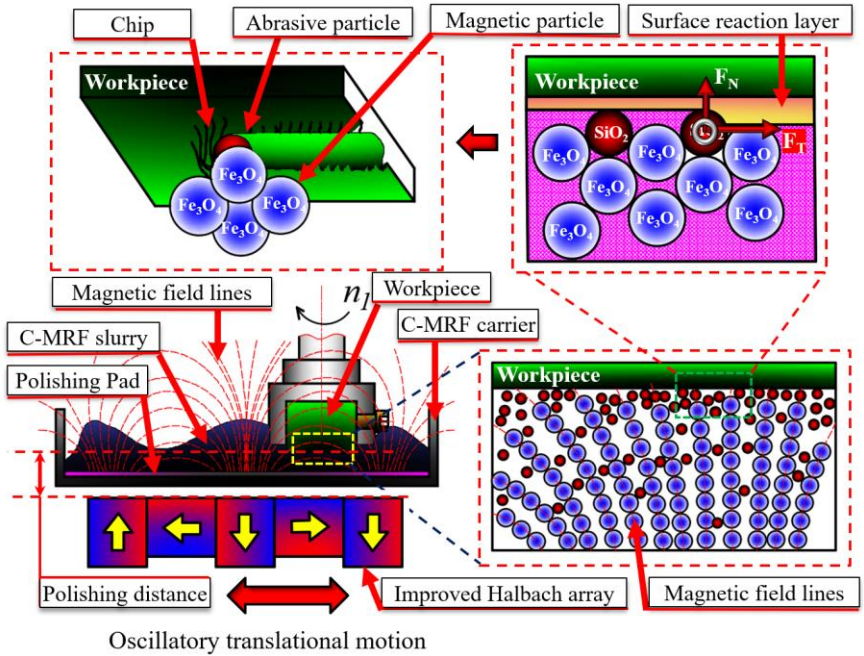


**Fig. 2.3** MRF polishing principle and machining residue removal mechanism with improved Halbach array

Under the influence of the magnetic field, the non-magnetic SiO<sub>2</sub> abrasive particles are pushed to the surface of the Ti-6Al-4V workpiece as shown in Fig. 2.3, generating a tangential force  $F_T$  and a normal force  $F_N$  acting on the workpiece surface. When the nanometer-sized SiO<sub>2</sub> abrasive particles move

relative to the workpiece, the combination of the rotational speed of the workpiece generated by the machine spindle and the reciprocating motion of the Halbach array enables the MRF ribbon to remove a very thin layer of workpiece material. During the polishing process, the semi-solid MRF ribbon consisting of  $\text{Fe}_3\text{O}_4$ ,  $\text{SiO}_2$  particles, oxidant  $\text{H}_2\text{O}_2$ , purified water and malic acid always maintains contact with the workpiece. As the MRF ribbon moves, new abrasive particles and magnetic particles are continuously formed due to the redistribution of the MRF strip in the polishing zone created by the slider crank mechanism. This helps to improve the surface finish of the material during the polishing process with the improved Halbach array.

#### **2.4. Magnetic field and kinetic analysis of $\text{Fe}_3\text{O}_4$ magnetic particles under the effect of modified Halbach array**

The magnetic field lines, magnetic flux density and magnetic force are improved in the proposed modified Halbach array. The magnetic flux density distribution and changes in the components are provided visually by 3D images. The material parameters are set in COMSOL multiphysics software to provide the coercive force and magnetization. The proposed simulation results have been verified by a magnetic flux meter.

#### **2.5. Analysis of the influence of $\text{Fe}_3\text{O}_4$ magnetic particles and $\text{SiO}_2$ abrasive particles under the effect of the improved Halbach magnetic field**

This enhanced magnetic field effect increases the hardness of the MRF ribbon, along with a stronger polishing force, significantly increasing the polishing efficiency. The results obtained show that the magnetic field analysis results during the polishing process are equivalent to the measured values as described in Fig. 2.4. When the improved Halbach array performs reciprocating movements, it creates MRF ribbons that move evenly on the machined surface, continuously supplying new  $\text{Fe}_3\text{O}_4$  magnetic particles and  $\text{SiO}_2$  abrasive particles, contributing to maintaining high polishing efficiency.

The force exerted on the  $\text{Fe}_3\text{O}_4$  magnetic particles generated by the magnetic fluxes obtained from the simulation results is illustrated in Fig. 2.5a. The maximum force exerted on the  $\text{Fe}_3\text{O}_4$  magnetic particles is observed at the adjacent edges of the magnet. Magnetic particles with high force values tend to move away from the workpiece surface and towards the Halbach array. The results shown in Fig. 2.5b show that different force values are present at different positions. However, all positions show that the  $\text{SiO}_2$  abrasive particles tend to move more towards the machined surface in MRF polishing processes with improved Halbach arrays.

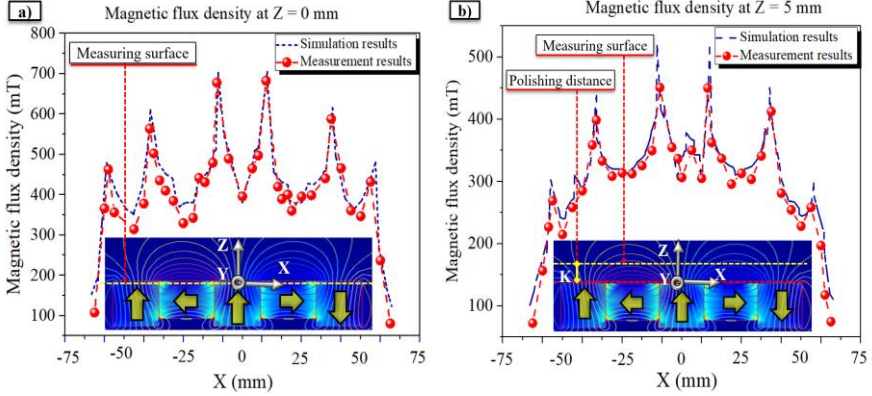


**Fig. 2.4** Measurement and simulation results of magnetic flux measured in the X direction

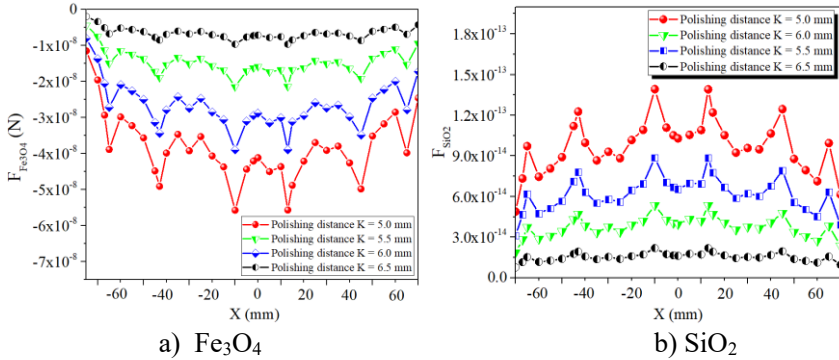


**Fig. 2.5** Magnetic force acting on  $\text{Fe}_3\text{O}_4$  magnetic particles and  $\text{SiO}_2$  abrasive particles under the effect of improved Halbach array

## 2.6. Establishment of polishing force model for polishing process with round-trip translational Halbach array

When considering the round-trip translational motion generated by the slider crank mechanism, the Halbach array moves round-trip translationally in the x direction, creating MRF ribbons moving round-trip translationally on the surface of the Ti-6Al-4V workpiece. Fig. 2.6 illustrates the displacement range in the x direction on the workpiece surface, generated by the action of the slider crank mechanism.

When the slider crank mechanism moves, the normal force and dynamic tangential force generated by the Halbach array at time t are determined by:

$$F_N = F_{s_0}(t) = \left( \frac{\mu_0 G R^5 \rho^2}{(R+s)^2} \iint_A (H^2 \chi_m^2) dA \int_{-\frac{\pi}{2}}^{\frac{\pi}{2}} \sum_{k=1}^{n-1} \left[ \frac{\sqrt{2} E_k}{2\sqrt{\pi \epsilon}} e^{\frac{1}{2} \left( \frac{\alpha - \theta}{\epsilon} \right)^2} \cos^5 \alpha \right] d\alpha \right) (s(t)) \quad (2.36)$$

$$\begin{aligned}
F_T &= F_{\tau_0}(t) + F_{\tau_i} = F_{\tau_0}(t) + PXma \\
&= \left( \frac{\mu_0 GR^5 \rho^2}{(R+s)^2} \iint_A (H^2 \chi_m^2) dA \int_{-\pi}^{\frac{\pi}{2}} \sum_{k=1}^{n-1} \left[ \frac{\sqrt{2} E_k}{2\sqrt{\pi \varepsilon}} e^{\frac{1}{2} \left( \frac{\alpha - \theta}{\varepsilon} \right)^2} \sin \alpha \cos^4 \alpha \right] d\alpha \right) (s(t)) + PXma
\end{aligned} \quad (2.37)$$

The MRF ribbon surface, when in contact with the Ti-6Al-4V workpiece, exerts a significant force on the workpiece surface, contributing to the effective removal of residual machining material. Under the action of the slider crank mechanism, the Halbach array moves in the x direction, resulting in the formation and movement of MRF ribbon strips following the movement of the Halbach array. The normal force, which depends on the interaction between the magnetic field of the Halbach array and the workpiece surface, is calculated by equation (2.36), while the tangential force, which is affected by the displacement speed and the mass of the abrasive grains, is determined by equation (2.37). These two forces combine to create cutting effects, which effectively remove residual machining material from the workpiece surface, while maintaining the stability of the magnetic chain and abrasive grains during the polishing process. The variation of these forces over time and the movement of the slider crank mechanism will directly affect the performance and polishing quality of the MRF system.

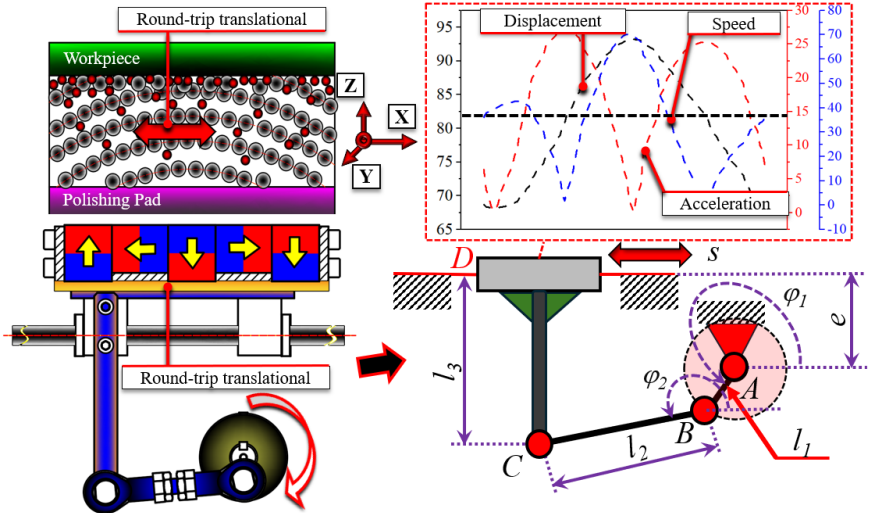


**Fig. 2.6** Motion characteristics of MRF ribbon under the action of translational Halbach array

## 2.7. Conclusion of Chapter 2

This chapter analyzes the disc-type MRF polishing principle and viscosity characteristics. An improved method using Halbach array is proposed to

concentrate the magnetic force in the polishing zone. The magnet configurations are designed, evaluated, and optimized with a size of  $25 \times 30$  mm, achieving a minimum magnetic moment of  $28.09 \text{ fAm}^2$ , a magnetic field of  $150 \times 135 \text{ mm}^2$ , and a magnetic flux density of  $2.05 \text{ T}$ .

During the polishing process, an MRF ribbon is formed at the contact point between the magnets, creating high pressure and large stiffness. The magnetic force analysis shows that the magnetic field distribution affects the abrasive and magnetic particles. In addition to the optimization of the Halbach array, this chapter also studies the magnetic force acting in the polishing zone.

Finally, a mathematical model is built to calculate the polishing force in the modified Halbach array with a round-trip motion. The optimized configuration enhances the magnetic force on  $\text{Fe}_3\text{O}_4$  and  $\text{SiO}_2$  particles, improving the material removal capacity and surface quality of Ti-6Al-4V.

### **CHAPTER 3**

#### **EXPERIMENTAL DESIGN OF MAGNETORHEOLOGICAL POLISHING USING IMPROVED HALBACH ARRAY FOR MACHINING Ti-6Al-4V ALLOY**

In this chapter, the following main contents are carried out:

#### **3.1. Objectives and requirements of experimental research**

##### ***Objectives:***

The experimental system was built to verify the feasibility of the MRF polishing model with the reciprocating Halbach array. Single-factor experiments were established to evaluate the effects of workpiece rotation speed, polishing distance, round-trip stroke of the Halbach array and MRF solution volume on polishing efficiency.

Experiments were conducted to evaluate the effects of pH concentration and  $\text{H}_2\text{O}_2$  oxidant content on the polishing efficiency of Ti-6Al-4V alloy, thereby determining the optimal conditions.

Experimental results show that the MRF model with the improved Halbach array helps to improve polishing efficiency, improve surface quality and material removal ability, affirming the potential application in precision machining of Ti-6Al-4V alloy.

##### ***Requirements:***

- The system should be designed for ease of fabrication, installation and operation, and easy integration with existing laboratory equipment.
- The Halbach array is controlled by a slider crank mechanism, which should maintain a stable magnetic force, optimize material removal and improve surface roughness.
- The system design should ensure stable operation, allowing flexible adjustment of technological parameters such as rotation speed, polishing distance and movement of the Halbach array.



### 3.2. Experimental system setup

#### 3.2.1. Machining machine

In this thesis, polishing experiments were carried out on a DMU50 5-axis milling machine, an advanced high-precision machining equipment. This is an important factor in the application of magnetic polishing technology, where surface quality and stability during machining play a key role.



**Fig. 3.1** Image of experimental equipment for polishing Ti-6Al-4V alloy MRF on 5-axis CNC machine DMU50

#### 3.2.2. Materials

In the experimental setup, Ti-6Al-4V workpieces with length, width, and height dimensions of  $32 \times 32 \times 15$  mm, respectively, were used in MRF polishing experiments with a modified Halbach plate with material parameters as described in Table 3.1. The surface of the Ti-6Al-4V workpiece before polishing was ground with a Ra of approximately 500 nm. The volume of MRF solution used in the MRF polishing processes was set at 500 mL. The specific composition is described in Table 3.2. SiO<sub>2</sub> abrasive particles (with an average particle size of 300 nm) were provided by Luoyang Tongrun Info Technology. The magnetic particles used were Fe<sub>3</sub>O<sub>4</sub> with an average particle size of 1  $\mu$ m provided by Changsha Zhonglong Chemical Company. The purified water used in the polishing processes was provided by Fisher Scientific Korea. With the MRF solution showing high performance and quality at low pH, the pH was set at 4 with malic acid (56%).

**Table 3.1** Chemical composition of Ti-6Al-4V alloy [105]

Ingredients	Ti	Al	V	Fe	C	N	H	O
Content (%)	-	5.5÷6.8	3.5÷4.5	0.30	0.1	0.05	0.015	0.20



**Table 3.3** Composition of MRF solution with SiO<sub>2</sub> abrasive particles and Fe<sub>3</sub>O<sub>4</sub> magnetic particles used

No.	Characteristics	Parameters	Volume (%)	Manufacturer
1	Abrasive (SiO <sub>2</sub> )	300 nm	10 Vol%	Luoyang Tongrun Info Technology Co., Ltd.
2	Magnetic particle (Fe <sub>3</sub> O <sub>4</sub> )	1 $\mu$ m	30 Vol%	Changsha Zhonglong Chemical Co., Ltd.
3	Oxidizer (H <sub>2</sub> O <sub>2</sub> )	-	4 Vol%	Shanghai Arkema Hydrogen Peroxide Co., Ltd.
4	Acid Malic	pH = 4	-	Shanghai Aladdin Biochemical Technology Co., Ltd.
5	Pure water	-	40-45 Vol%	Fisher Scientific Korea Co., Ltd.

### 3.2.3. Measuring equipment

In this study, the magnetic field strength, surface roughness, cutting force and cutting tool wear were measured using a Mitutoyo Surftest JS-210 roughness measuring device; a Kistler 9139AA force measuring device and a Keyence VHX-7000 optical microscope.



**Fig. 3.2** Magnetic field measuring devices KT-101, Kistler 9139AA and VHX-7000

### 3.3. Establishment of single-factor experiments

To evaluate the influence of process parameters ( $V_c$ ,  $f_z$ ,  $a_p$ ) on surface roughness  $R_a$ , cutting force  $F_c$  and tool back wear  $V_b$ , Taguchi matrix L27 was selected for experimental study.

#### 3.3.1. Experimental matrix

To evaluate the surface quality and material removal ability when polishing Ti-6Al-4V alloy MRF by Halbach array, experiments were designed based on the polishing conditions and process parameters listed in Table 3.4.

**Table 3.4** Polishing parameters with improved Halbach array

Level	Workpiece speed	Halbach array dual-stroke	Polishing distance	MRF volume
1	200 rpm	15 rpm	1 mm	200 ml
2	300 rpm	20 rpm	1.5 mm	300 ml
3	400 rpm	25 rpm	2 mm	400 ml
4	500 rpm	30 rpm	2.5 mm	500 ml

Under the influence of the magnetic field generated by the Halbach array, the structure of the  $\text{Fe}_3\text{O}_4$  magnetic particle clusters in the MRF solution increased, as shown in Fig. 3.3, when these particles arranged in chains along the magnetic field lines. The gradient of the magnetic field generated by the modified Halbach array caused the magnetic particles to adhere tightly to the Polishing Pad and move back and forth in synchronization with the Halbach array.

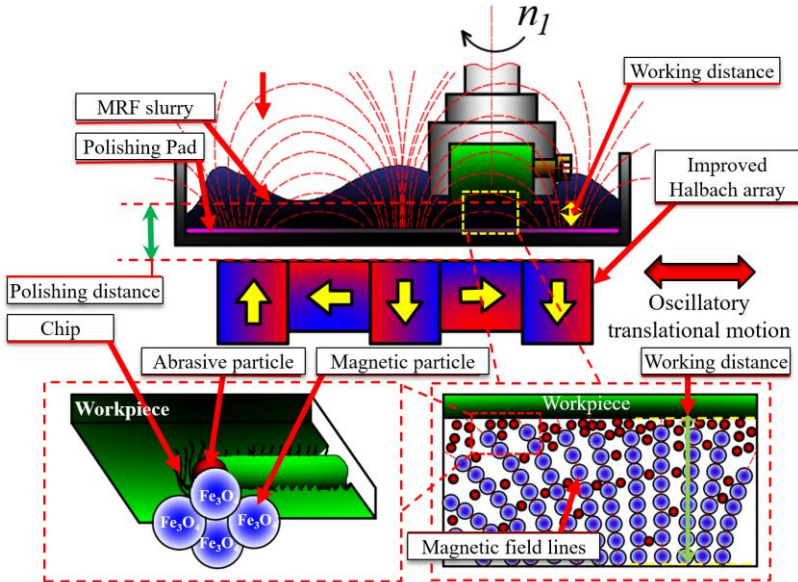


**Fig. 3.3** Schematic diagram of MRF polishing with improved Halbach array

Under the influence of the applied magnetic field, the magnetic particles are attracted to the Halbach array while the non-magnetic  $\text{SiO}_2$  abrasive particles are pushed towards the Ti-6Al-4V workpiece surface as illustrated in Fig. 3.8. In addition, these  $\text{SiO}_2$  abrasive particles are held tightly by the  $\text{Fe}_3\text{O}_4$  magnetic

particles in the MRF ribbon, forming a cutting force acting on the workpiece surface.

The polishing procedures for CMP and MRF were performed as described in Table 3.5 to determine the most efficient polishing method for Ti-6Al-4V blanks. The polishing time was adjusted to 20, 40, 60, 80, and 100 min, with a polishing distance of 5 mm and the rotation speed of the motor to create reciprocating motion for the MRF ribbon was set at 25 rpm.

**Table 3.5** MRF polishing mixture composition

Polishing slurry	Acid Type	Percentage of oxidant	Abrasive	Slurry volume	Abrasive grain volume
CMP-1	HOOC-CH <sub>2</sub> -CH(OH)-COOH	2 %	SiO <sub>2</sub>	200 ml	40 %
CMP-2	H <sub>3</sub> PO <sub>4</sub>	2 %	SiO <sub>2</sub>	200 ml	40 %
CMP-3	H <sub>2</sub> SO <sub>4</sub>	2 %	SiO <sub>2</sub>	200 ml	40 %
MRF -1	HOOC-CH <sub>2</sub> -CH(OH)-COOH	2 %	Fe <sub>3</sub> O <sub>4</sub> -SiO <sub>2</sub>	200 ml	40 %
MRF -2	H <sub>3</sub> PO <sub>4</sub>	2 %	Fe <sub>3</sub> O <sub>4</sub> -SiO <sub>2</sub>	200 ml	40 %
MRF -3	H <sub>2</sub> SO <sub>4</sub>	2 %	Fe <sub>3</sub> O <sub>4</sub> -SiO <sub>2</sub>	200 ml	40 %

Single factor experiments were conducted to study the influence of each individual factor on the polishing efficiency and surface quality of Ti-6Al-4V alloy. In these experiments, each process parameter was varied while the experimental conditions with other process parameters were kept constant. The aim of these experiments was to determine the optimal process parameters for the polishing solution and to find the most suitable polishing time for the proposed MRF polishing model.

### 3.4. Polishing pressure exerted by Halbach array on magnetic ribbon (MRF)

The pressure and trace exerted by MRF ribbon on Ti-6Al-4V workpiece surface during magnetic polishing with modified Halbach array are shown in Fig. 3.4. The pressure of MRF ribbon is concentrated at the boundary area (C) between the magnets, indicating high material removal ability at this boundary area. At this boundary area, due to the presence of high magnetic force and gradient, Fe<sub>3</sub>O<sub>4</sub> magnetic particles are concentrated in this area. Therefore, MRF ribbon with high pressure and magnetic force is formed and acts on SiO<sub>2</sub> abrasive particles, ensuring effective removal of residual machining material.

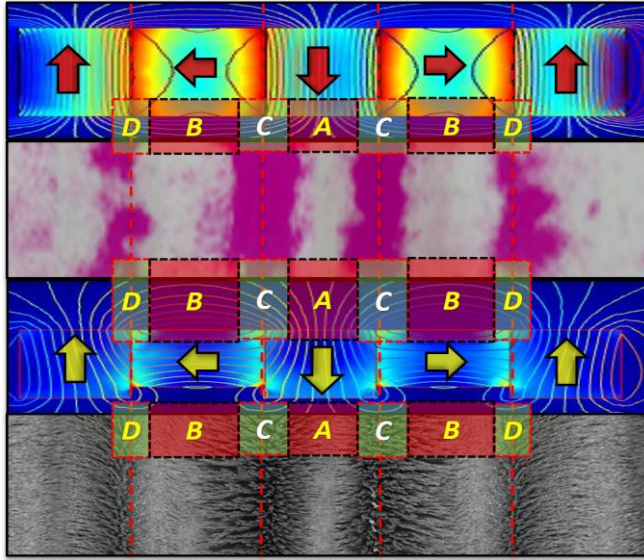


**Fig. 3.4** Pressure applied to the MRF ribbon during the polishing process

### 3.5. Analysis and selection of acids and abrasives for magnetic polishing process

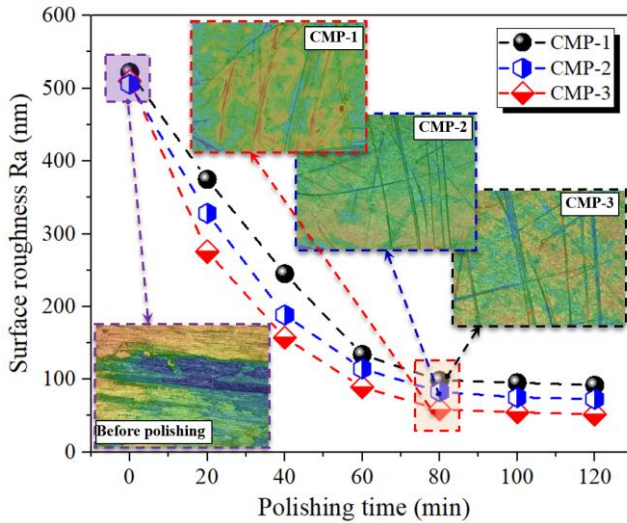


**Fig. 3.5** Surface roughness of Ti-6Al-4V workpiece over time by CMP processes

Polishing methods with different MRF solutions are shown in Table 3.5, with surface roughness changes with different polishing times as shown in Fig.

3.6. Notably, the impact of different acids on the surface quality in the proposed MRF polishing process is negligible. At the same time, the surface quality has been significantly improved compared to the CMP polishing process as shown in Fig. 3.5, with small scratches and surface roughnesses of 10 nm, 9 nm and 7 nm achieved when using malic acid ( $C_4H_6O_5$ ), phosphoric acid ( $H_3PO_4$ ) and sulfuric acid ( $H_2SO_4$ ), respectively. The analysis results as shown in Figs. 3.5 and 3.11 show that an effective MRF polishing process has been established, using a reciprocating Halbach array generating a strong magnetic field. This approach proved to be superior to the conventional CMP polishing process in improving polishability.

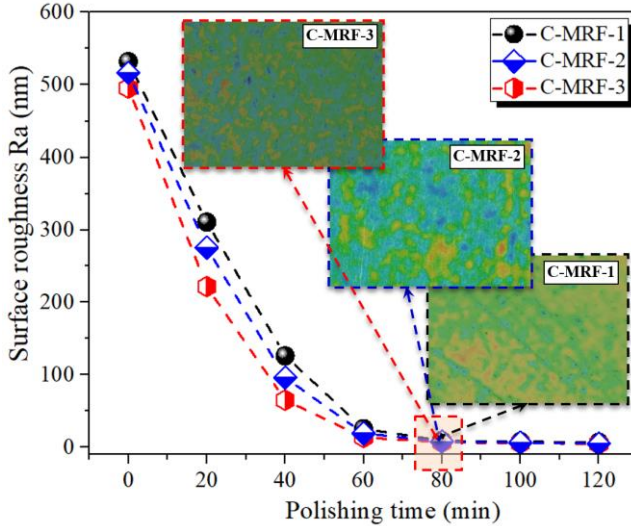


**Fig. 3.6** Surface roughness of Ti-6Al-4V workpiece obtained with different time and MRF solution

In the CMP polishing process, strong and weak acids, such as malic acid, phosphoric acid and sulfuric acid, are used, resulting in different surface roughness results, with stronger acids achieving lower roughness. However, the MRF polishing process, incorporating the Halbach plate, strikes an ideal balance between mechanical and chemical factors. This balance not only enhances material removal but also ensures high surface quality.

### 3.6. Analysis of polishing performance of Ti-6Al-4V alloy under different pH concentrations in MRF solution

The MRF solution was composed of  $Fe_3O_4$  magnetic particles and  $SiO_2$  abrasive particles with a volume ratio of 40%, purified water, and the pH concentration was set in the range of 4 to 10. The results presented in Fig. 3.7a show that as the pH increases, the rate of removing excess machining material decreases. Especially at the pH level of 10, the material removal capacity is the

lowest when polishing Ti-6Al-4V alloy with MRF. The description in Fig. 3.7b shows that the surface quality of Ti-6Al-4V workpiece tends to decrease as the pH increases. The experimental results show that when the pH level reaches 4, the surface quality is the best. However, when the pH level increases to 7, the number of scratches on the surface is significantly higher, resulting in a rougher surface quality obtained. When sodium hydroxide (NaOH) was added to bring the pH above 7, there was a slight improvement in surface quality, but it was not significant.

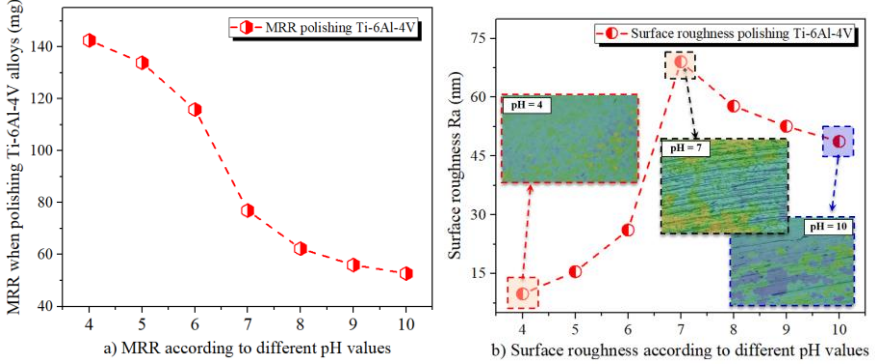


**Fig. 3.7** Surface roughness of Ti-6Al-4V workpiece over time by CMP processes

When the pH increases to 10, the rate of removal of residual machining material decreases sharply, although the surface quality is slightly improved compared to pH 7. At high pH, a durable oxide film forms on the titanium alloy surface, which protects the surface from negative impacts during polishing, which is not beneficial to the MRF polishing process. However, when the pH drops below 4, the environment becomes harmful, so studies have set the pH limit between 4 and 10 to balance polishing performance and environmental protection.

### 3.7. MRF polishing performance of Ti-6Al-4V alloy according to $H_2O_2$ oxidant content

During the polishing kinetics test of the influence of  $H_2O_2$  oxidant on Ti-6Al-4V alloy, an MRF solution combining 40% by volume of abrasive and  $Fe_3O_4-SiO_2$  magnetic particles was prepared. The pH was maintained at 4 and different concentrations of  $H_2O_2$  oxidant were introduced into the polishing sequences. Fig. 3.8a and b illustrate the surface quality and material removal rate (MRR), showing the changes in MRR of Ti-6Al-4V alloy and surface quality corresponding to different concentrations of  $H_2O_2$  oxidant.

When  $H_2O_2$  is added to the solution, an oxide film is rapidly formed on the surface of the Ti alloy, which helps the abrasive grain to work more effectively,



thereby increasing the material removal capacity and improving the surface quality. However, when the  $H_2O_2$  concentration increases to 3.5% by volume, the rate of removing the workpiece residue decreases, which may be due to the rapid development of the oxide film on the surface, making it difficult for the abrasive grain to penetrate the oxide film to remove the workpiece residue. In addition, a small amount of oxide may accumulate in the MRF slurry and on the polishing pad, causing a decrease in surface quality when the  $H_2O_2$  concentration exceeds 1.5% by volume.

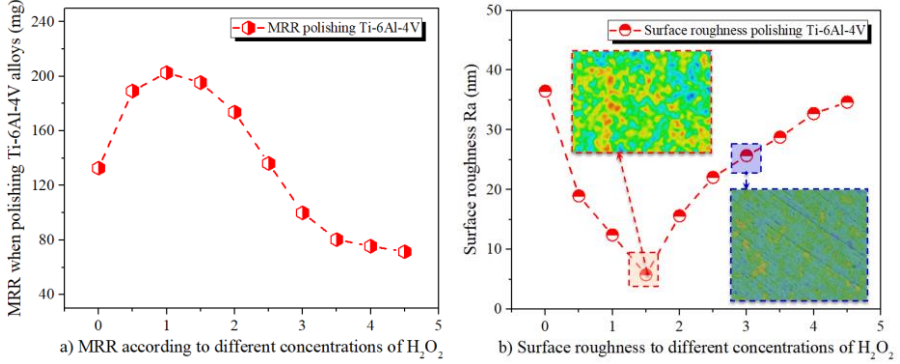


**Fig. 3.8** MRF polishing efficiency of Ti-6Al-4V alloy according to  $H_2O_2$  concentration

### 3.8. MRF polishing capability with improved Halbach array

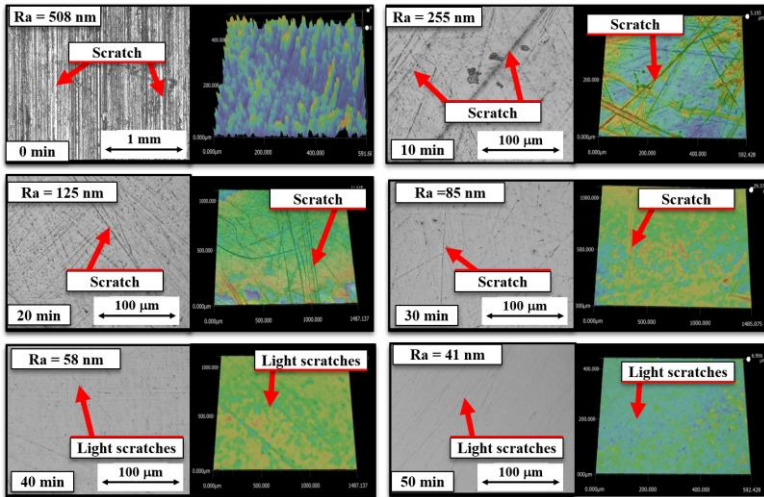


**Fig. 3.9** Surface morphology of Ti-6Al-4V blanks according to MRF polishing time with reciprocating Halbach array

The changes in the surface morphology of the Ti-6Al-4V workpiece over time are shown in Fig. 3.9. The deep dents and surface dents left by the initial grinding process are gradually eliminated, replaced by a surface with significantly improved roughness. The initial surface has a roughness of about 500 nm and is polished at a polishing distance of 5 mm. The polishing times required to achieve surface roughness are 255, 125, 85, 58 and 41 nm for 10, 20, 30, 40 and 50 minutes, respectively. After 80 minutes of polishing, the surface appears with very small scratches and pits that are difficult to observe, along with a mirror-like surface with a roughness of Ra of 7 nm. This shows that with the MRF polishing model with the improved Halbach array, the polishing efficiency is high, and the surface roughness reaches the nanometer level.

### 3.9. Conclusion of chapter 3

- The surface quality and material removal rate (MRR) of Ti-6Al-4V workpieces during MRF polishing were affected by pH and H<sub>2</sub>O<sub>2</sub> concentration.
- As pH increased, the surface gloss and MRR decreased, while higher H<sub>2</sub>O<sub>2</sub> concentrations increased the MRR, reaching a maximum at 1 vol%.
- After 80 min of polishing with the modified Halbach array, the surface roughness reached Ra 7 nm, demonstrating the high efficiency of the proposed method.

## CHAPTER 4 RESULTS AND DISCUSSION

### 4.1. Experimental setup to verify the cutting force model

Fig. 4.1 shows the experimental setup for MRF polishing using a reciprocating Halbach array driven by a slider crank mechanism. The polishing experiments were performed with an initial roughness of approximately 500 nm on a Ti-6Al-4V alloy workpiece of 32×32×15 mm. In these experiments, the MRF volume was set to 400 ml, consisting of Fe<sub>3</sub>O<sub>4</sub> magnetic particles (1 μm, 36% by volume), SiO<sub>2</sub> abrasive particles (300 nm, 8% by volume), and 2% H<sub>2</sub>O<sub>2</sub> by volume with malic acid adjusted to a pH of 4. The force signals were measured using a Kisler 9139AA force sensor with a resolution of 0.01 N, which was mounted below the MRF polishing device.

Based on the experimental data presented in Table 4.1, the values of  $\varepsilon$  and  $\theta$  were determined to be 0.2508 and 0.5128, respectively. Experiments were conducted under different conditions to verify the reliability of the proposed  $F_T$  and  $F_N$  models including: MRF volume, polishing distance (K) and workpiece rotation speed. Various technological parameters were selected and their corresponding levels are presented in Table 4.2.

Fig. 4.2 shows the measured values of  $F_T$  and  $F_N$  during the polishing of Ti-6Al-4V material with magnetic particles and Fe<sub>3</sub>O<sub>4</sub> and SiO<sub>2</sub> abrasive



particles. In the polishing processes using Halbach array driven by a slider-crank mechanism, it can be seen that both the normal force  $F_T$  and the tangential force  $F_N$  increase as the number of double passes increases from 15 to 25.

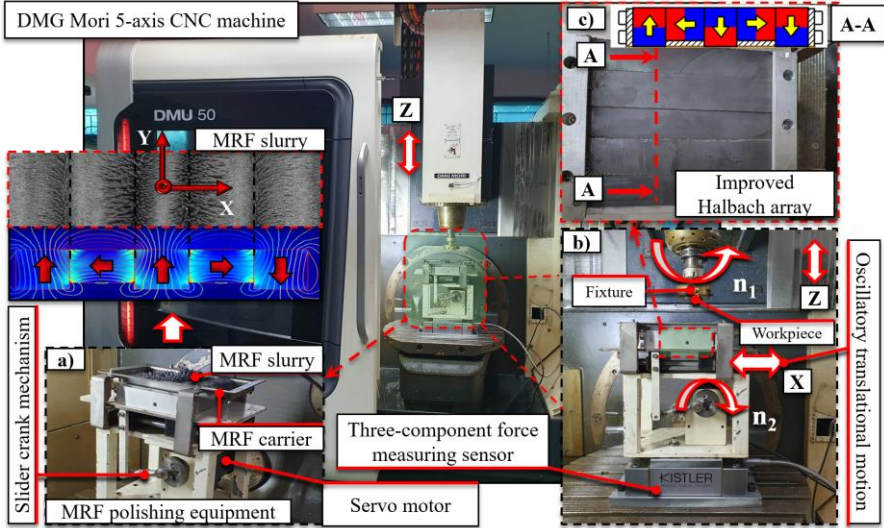


**Fig. 4.1** MRF polishing device with reciprocating Halbach array

**Table 4.1** Experimental parameters determining coefficients  $\varepsilon$  and  $\theta$

No.	Technical specifications			20 double trips of the Halbach array			30 double trips of the Halbach array		
	Vol. MRF (ml)	Workpiece speed (rpm)	Polishing distance K (mm)	$F_T$ (N)	$F_N$ (N)	$MRR$ (mg/h)	$F_T$ (N)	$F_N$ (N)	$MRR$ (mg/h)
1	250	200	1	27.8	16.4	85.4	34.2	20.4	100.6
2	450	200	1	38.2	23.2	114.2	48.1	28.3	139.5
3	600	200	1	45.9	28.0	136.3	57.1	35.0	165.7
4	450	400	1.4	32.9	25.7	108.5	40.7	31.7	132.2
5	450	400	1.8	28.5	17.9	90.8	35.8	22.5	117.6
6	450	400	2.2	22.9	15.8	79.4	28.1	19.7	93.5
7	450	250	1.4	26.2	16.9	84.2	33.6	20.8	105.1
8	450	450	1.4	29.1	18.0	94.3	35.2	21.9	114.3
9	450	650	1.4	31.4	19.5	105.3	39.4	25.1	129.5

**Table 4.2** Experimental validation of  $F_T$  and  $F_N$  polishing force models

Technical specifications	Experimental order					
	1	2	3	4	5	6

MRF volume (ml)	200	225	250	275	300	325
Workpiece speed (vòng/phút)	200	300	400	500	600	700
Polishing distance K (mm)	1	1.2	1.4	1.6	1.8	2

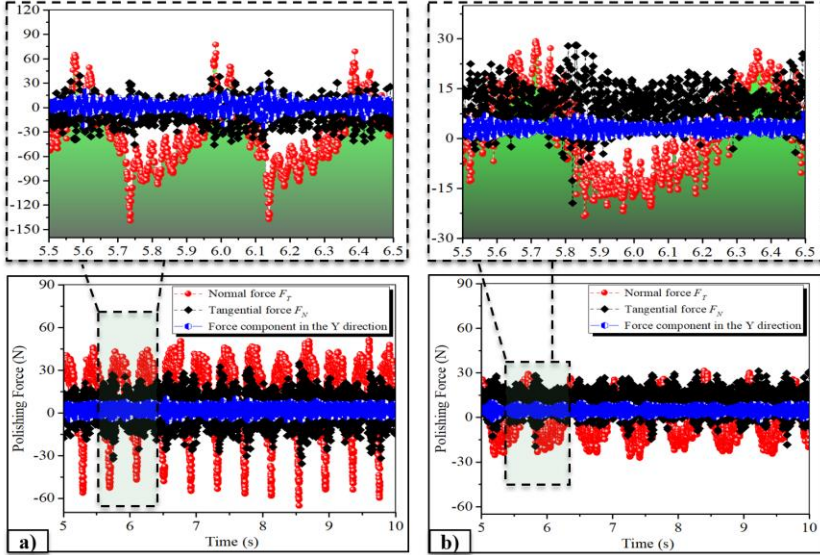


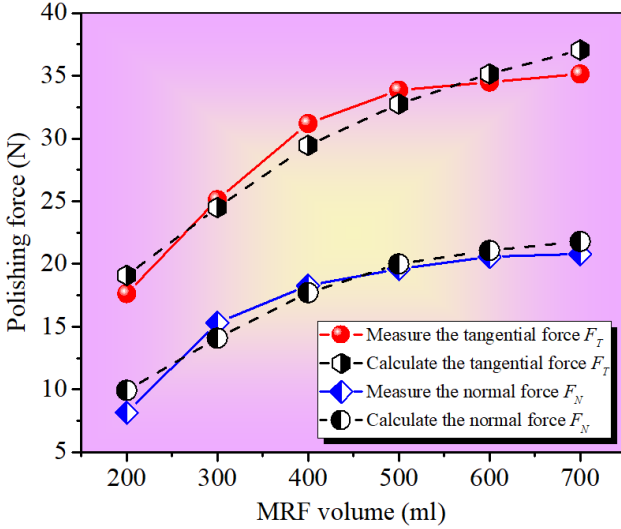
**Fig. 4.2**  $F_T$  and  $F_N$  force components change with double stroke of Halbach array: (a) 25 double strokes per minute, (b) 15 double strokes per minute

#### 4.2. Tangential and normal forces in magnetic polishing using reciprocating Halbach arrays

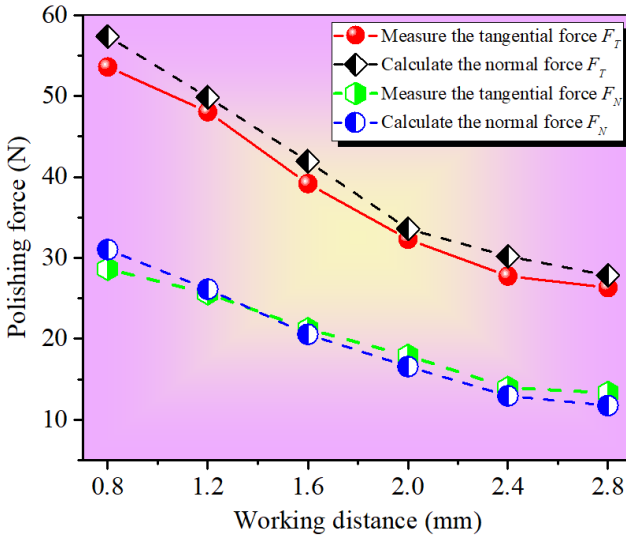
Fig. 4.3 illustrates the effect of MRF solution volume on the force components  $F_T$  and  $F_N$  during polishing using reciprocating Halbach arrays. The results show that increasing the MRF volume, corresponding to higher magnetic particle content, leads to increases in both  $F_T$  and  $F_N$ . As the MRF volume increases, more magnetic particle chains participate in the polishing process, resulting in denser MRF bands with higher hardness. The increased MRF ribbon stiffness and cutting efficiency result in higher polishing forces when moving relative to the Ti-6Al-4V workpiece.

Increasing the polishing distance will result in a decrease in magnetic force, thereby reducing the force exerted on the workpiece due to the decreased stiffness of the MRF ribbon as illustrated in Fig. 4.4. Fig. 4.5 illustrates the effect of changing the workpiece speed on the polishing force components  $F_T$

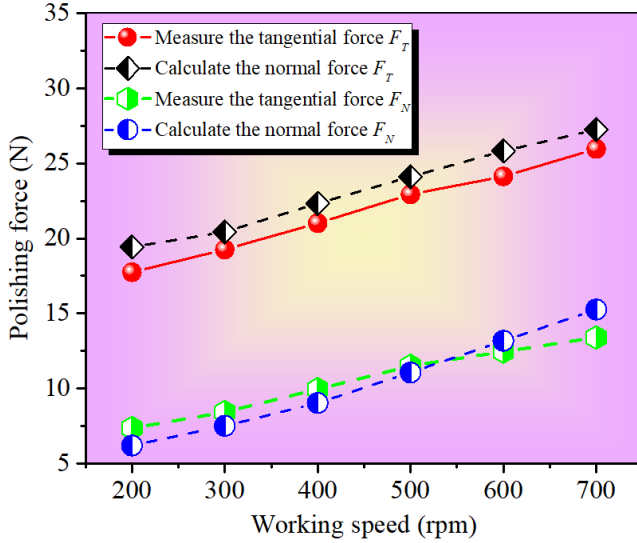
and  $F_N$ . The data indicate that increasing the workpiece speed increases the relative motion between the workpiece and the MRF polishing ribbon, thereby increasing the polishing force.



**Fig. 4.3** Theoretical and experimental results of determining polishing force  $F_T$  and  $F_N$  when changing the volume of MRF slurry



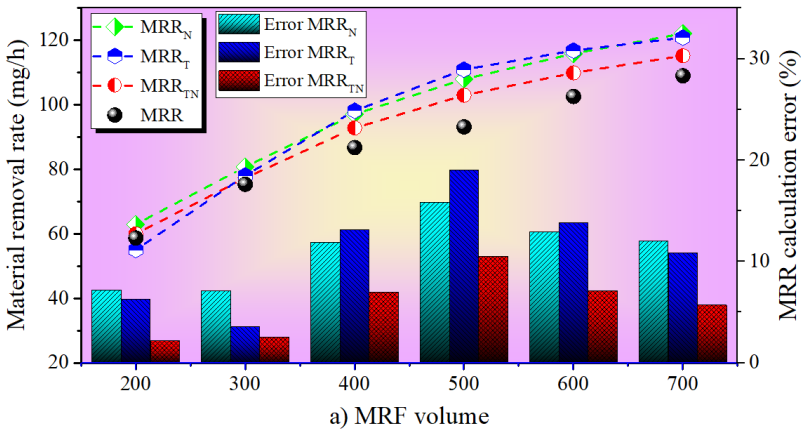
**Fig. 4.4** Polishing force  $F_T$  and  $F_N$  change with polishing distance  $K$



**Fig. 4.6** Polishing force  $F_T$  and  $F_N$  change with workpiece speed

#### 4.3. Material removal model in magnetic polishing using round-trip translational Halbach array

Fig. 4.7 illustrates the model for predicting the material removal rate (MRR) and the error between the theoretical MRR value and the experimental data. The results show that the removal rate of the residual workpiece material increases with higher MRF concentration and polishing speed, but decreases with increasing working distance.



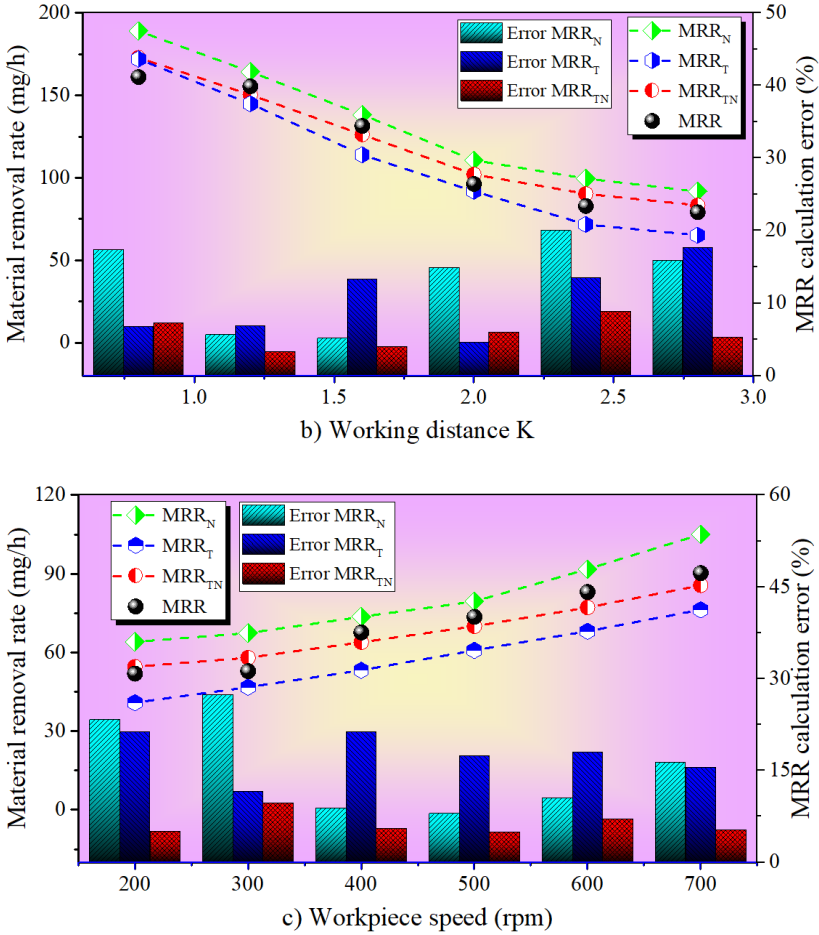


**Fig. 4.7** Error values of MRRNT, MRRT and MRRN compared to experiment (MRR)

The MRR prediction model for Ti-6Al-4V workpieces during MRF polishing using a translational Halbach array shows that the tangential force has a greater influence than the normal force. The prediction results and errors show that the improved MRR<sub>TN</sub> model, which incorporates both  $F_T$  and  $F_N$ , provides higher accuracy than previous models that only consider one of these two force components. The improved accuracy of the MRR prediction model is important in the development of a polishing system using a translational Halbach array, when taking into account the relative motion trajectory between the MRF ribbon and the workpiece. This study will contribute significantly to

the accurate prediction of the surface quality of Ti-6Al-4V workpieces for future studies.

#### 4.4. Orthogonal Experimental Setup

In addition to studying each individual factor, orthogonal experiments were applied to the polishing process of Ti-6Al-4V alloy to find out the optimal technological parameters and create a basis for scientific analysis of the results as described in Tables 4.3 and 4.4. These tests were systematically organized according to the orthogonal table L16.

**Table 4.3** Elements and levels in the proposed MRF polishing process

Level	Halbach array dual-stroke	Polishing distance ( <i>mm</i> )	Workpiece speed ( <i>rpm</i> )	MRF volume ( <i>ml</i> )
1	15 Dual Stroke	1	200	200
2	20 Dual Stroke	1.5	300	300
3	25 Dual Stroke	2	400	400
4	30 Dual Stroke	2.5	500	500

**Table 4.4** Orthogonal MRF polishing experiments for Ti-6Al-4V alloy

No.	Dual Stroke Halbach array	Polishing distance	Workpiece speed	MRF volume	Ra ( <i>nm</i> )	MRR ( <i>mg</i> )
1	1	1	1	1	19	177.7
2	1	2	2	2	14	152.6
3	1	3	3	3	23	131.5
4	1	4	4	4	36	103.1
5	2	1	2	3	11	205.7
6	2	2	1	4	8	182.2
7	2	3	4	1	29	98.2
8	2	4	3	2	35	92.3
9	3	1	3	4	7	225.7
10	3	2	4	3	5	203.3
11	3	3	1	2	24	141.5
12	3	4	2	1	43	86.6
13	4	1	4	2	9	229.1
14	4	2	3	1	10	167.8
15	4	3	2	4	21	163.8
16	4	4	1	3	41	103.1

After completion, the results were analyzed using the range method to determine the order of influence of the main and secondary factors on the surface quality and material removal capacity, and to provide the optimal set of process parameters. MRF polishing experiments were performed with factors

affecting the surface roughness and material removal capacity, including the double stroke of the reciprocating Halbach plate (C1), polishing distance (C2), workpiece speed (C3), and MRF slurry volume (C4).

#### 4.5. Surface quality of MRF polishing with reciprocating Halbach array according to different process parameters

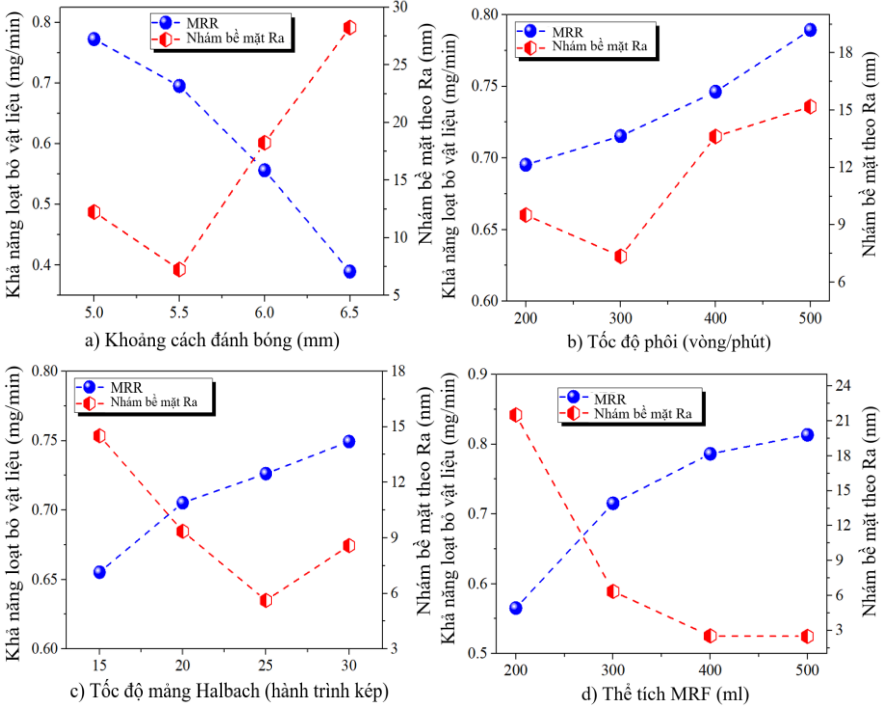


**Fig. 4.8** Effect of process parameters on surface quality and material removal capacity

The process parameters affecting the material removal capacity and surface roughness are illustrated in Fig. 4.8. When the polishing distance increased from 5 mm to 6.5 mm, the MRR decreased from 0.77 to 0.39 mg/min due to the decrease in magnetic field strength (Fig. 4.8a). Increasing the workpiece rotation speed from 200 to 500 rpm increased the MRR from 0.65 to 0.76 mg/min due to the increase in the number of contacts between the workpiece and the MRF ribbon (Fig. 4.8b). When the number of double strokes of the Halbach array increased, the MRR also increased from 0.66 to 0.73 mg/min due to the increased movement between the workpiece and the ribbon (Fig.

4.8c). The optimal MRF volume was 400 mL, resulting in an MRR of 0.86 mg/min without material waste (Fig. 4.8d).

The results are depicted in Fig. 4.10, which elucidates the influence indices ( $M_{ij}$ ) related to surface roughness and MRR after polishing Ti-6Al-4V alloy performed under different technological parameters, each of which is characterized by specific levels. When analyzing the surface roughness, it can be clearly seen from Fig. 4.9 that for factor C1, the lowest average  $M_{ij}$  value is observed at level 4, and factors C2, C3 and C4 exhibit levels 2, 3 and 4, respectively. Therefore, the optimal parameter combination to achieve the lowest surface roughness value is established as C1, C2, C3 and C4 at levels 4, 2, 3 and 4. On the contrary, in the context of MRR, a higher  $M_{ij}$  value indicates improved polishing efficiency. Therefore, the parameters associated with the highest machining material removal correspond to C1, C2, C3 and C4 at levels 4, 1, 2 and 4 as shown in Fig. 4.10.

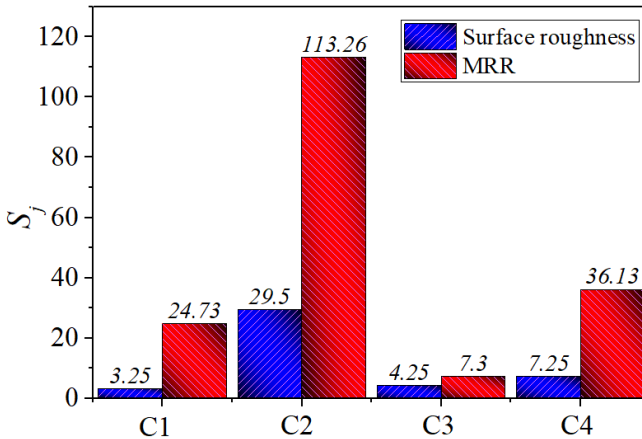


**Fig. 4.9** Corresponding  $S_j$  values of each factor

The surface morphology results are shown in Fig. 4.11, with four verification experiments showing that the surface roughness obtained with  $R_a = 1$  nm was significantly improved compared to the results from 16 sets of experiments using the orthogonal method. The verification experiments showed that the surface quality was significantly improved. The surface morphology observations during the verification experiments showed that only very small scratches appeared and the surface achieved a high gloss. The application of the MRF polishing process with a reciprocating Halbach array to the Ti-6Al-4V alloy, based on the orthogonal experiments, allowed the determination of the optimal parameters. The results of this verification process showed that the Ti-6Al-4V alloy surface achieved a high gloss and was superior to the orthogonal experiment, demonstrating the effectiveness of the polishing process in improving the surface quality and controlling scratches to a minimum level.



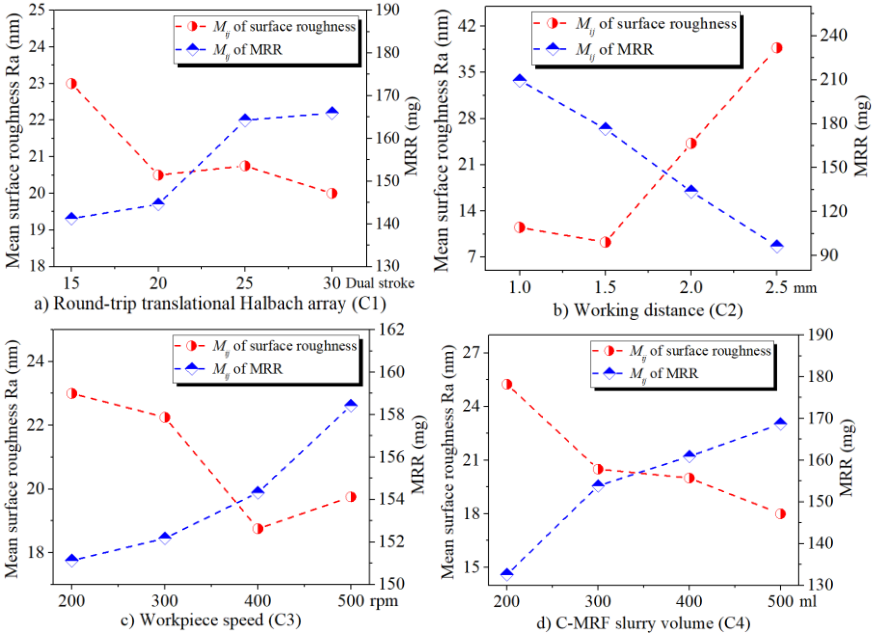


**Fig. 4.10**  $M_{ij}$  with Ra and MRR when polishing Ti-6Al-4V workpiece with MRF solution according to orthogonal experiments

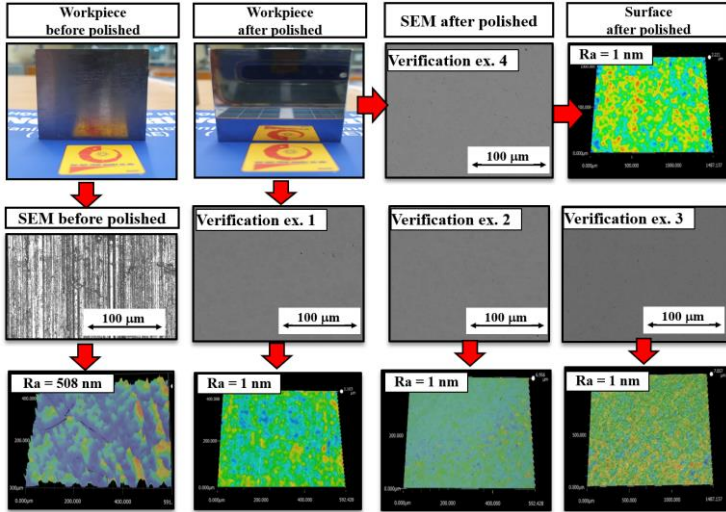


**Fig. 4.11** Surface of Ti-6Al-4V workpiece after MRF polishing with reciprocating Halbach array under optimal technological conditions

#### 4.6. Conclusion of Chapter 4

The environmentally friendly MRF polishing process was applied to Ti-6Al-4V alloy, in which the mathematical model of tangential force ( $F_T$ ) and normal force ( $F_N$ ) was experimentally verified with a translational Halbach array. The orthogonal experiment combined the range method to determine the optimal technological parameters, using an MRF solution consisting of  $\text{SiO}_2$ ,  $\text{Fe}_3\text{O}_4$ ,  $\text{H}_2\text{O}_2$  and malic acid. The results showed that the polishing force model achieved high accuracy (error below 16%), and the model predicted MRR more accurately when considering both  $F_T$  and  $F_N$ . The order of influence on surface roughness was polishing distance > MRF volume > workpiece rotation speed > Halbach array. The optimal parameters included 30 double strokes, polishing distance 1.5 mm, workpiece rotation speed 400 rpm, MRF volume 500 ml, helping to achieve  $R_a = 1 \text{ nm}$ .

#### DEVELOPMENT DIRECTION OF THE THESIS

The research topics that need to be continued are:

1. Using SEM, TEM, XRD to analyze surface changes during MRF polishing, clarify the chemical and mechanical mechanisms, thereby optimizing polishing materials and solutions.
2. Developing high-performance Halbach arrays for polishing complex surfaces (spherical, conical, microstructures), expanding MRF applications in aviation, medicine, and electronic components.
3. Applying genetic algorithms, machine learning, AI to optimize and predict surface quality, improve polishing efficiency and save resources.
4. Developing environmentally friendly MRF solutions, ensuring high performance, meeting strict environmental standards.
5. Expanding MRF for advanced materials such as ceramics, super-strong alloys, composites, enhancing technological potential in manufacturing requiring atomic-level precision.

## LIST OF PUBLISHED SCIENTIFIC WORKS

- [1] D. H. Tien and **T. N. Duy\***, "Novel magnetic field array optimization method for the chemical magnetorheological finishing of Ti-6Al-4V alloy with SiO<sub>2</sub> abrasive and Fe<sub>3</sub>O<sub>4</sub> magnetic particles," *The International Journal of Advanced Manufacturing Technology* (**SCIE Q1, IF 2.9**), vol. 134, no. 3, pp. 1395-1417, 2024/08/03 2024.
- [2] D. H. Tien and **N. D. Trinh\***, "Novel hybrid chemical magnetorheological fluid for polishing Ti-6Al-4V alloy," *Materials and Manufacturing Processes* (**SCIE Q1, IF 4.1**), vol. 39, no. 12, pp. 1798-1815, 2024/03/07 2024.
- [3] D. H. Tien, P. T. T. Thoa, N. Van Que, and **T. N. Duy\***, "Developing material removal rate from polishing force modeling via magnetorheological finishing using an improved Halbach array with a slider crank mechanism for Ti-6Al-4V alloy," *Materials Today Communications* (**SCIE Q1, IF 3.7**), vol. 45, p. 112360, 2025/04/01/ 2025.
- [4] **N. D. Trinh**, D. H. Tien, P. T. T. Thoa, N. Van Que, K. V. Quang, and N. T. Mai, "Circular Halbach array integrated using an abrasive circulating system during the ultra-precision machining of polymethyl methacrylate optical material," *International Journal of Lightweight Materials and Manufacture* (**SCOPUS Q1**), vol. 7, no. 6, pp. 793-808, 2024/11/01/ 2024.
- [5] **N. Duy Trinh et al.**, "A Novel Circulating Abrasive Flow Strategy Using Circular Halbach Array for Magneto-Rheological Finishing of Ti-6Al-4V," *Journal of Machine Engineering* (**SCOPUS Q2**), vol. 24, 03/13 2024.
- [6] D. H. Tien, **T. N. Duy**, and P. T. T. Thoa, "Applying GPR-FGRA hybrid algorithm for prediction and optimization of eco-friendly magnetorheological finishing Ti-6Al-4V alloy," *International Journal on Interactive Design and Manufacturing (IJDeM)* (**ISI Q2**), vol. 17, no. 2, pp. 729-745, 2023/04/01 2023.
- [7] **Trinh, N.D.**, N.M. Quang, L.T.P. Thanh, N.T. Tung, D.N. Hoanh, and N.N. Quan, *An advanced magnetic abrasive finishing with regenerative abrasive particles for polymethyl methacrylate material using a Halbach array*. Sādhana (**SCIE Q2**), 2025. **50**(2): p. 74.
- [8] **Duy, T.N.**, N.M. Quang, and N. Van Que, *Surface quality and material removal via viscosity-controlled Magnetorheological finishing Ti-6Al-4V using Fe<sub>3</sub>O<sub>4</sub>-SiO<sub>2</sub> abrasives and Halbach array*. Results in Engineering (**ISI Q1**), 2025. **26**: p. 105089.

## REFERENCES

- [1] G. Liu, D. Zhang, and C. Yao, "A modified constitutive model coupled with microstructure evolution incremental model for machining of titanium alloy Ti-6Al-4V," *Journal of Materials Processing Technology*, vol. 297, p. 117262, 2021/11/01/ 2021.
- [2] Y. Liu, D. Geng, Z. Shao, Z. Zhou, X. Jiang, and D. Zhang, "A study on strengthening and machining integrated ultrasonic peening drilling of Ti-6Al-4V," *Materials & Design*, vol. 212, p. 110238, 2021/12/15/ 2021.
- [3] N. Khanna, P. Shah, L. N. L. de Lacalle, A. Rodríguez, and O. Pereira, "In pursuit of sustainable cutting fluid strategy for machining Ti-6Al-4V using life cycle analysis," *Sustainable Materials and Technologies*, vol. 29, p. e00301, 2021/09/01/ 2021.
- [4] A. S. Kumar, B. G. Priyadarshini, B. Jahaziel, and V. Krishnaraj, "On the formation of Ti<sub>2</sub>AlN MAX phase coatings and improvement in tool life by superimposing on tungsten carbide cutting tool for machining Ti-6Al-4V alloys," *Journal of Manufacturing Processes*, vol. 107, pp. 210-225, 2023/12/01/ 2023.
- [5] R. Bammidi, D. Sreeramulu, H. Madivada, P. K. Rejeti, and M. Venkatesh, "Towards an understanding of Ti-6Al-4V machining and machinability," *Materials Today: Proceedings*, 2023/09/15/ 2023.
- [6] V. Zega *et al.*, "A 3D Printed Ti6Al4V Alloy Uniaxial Capacitive Accelerometer," *IEEE Sensors Journal*, vol. 21, no. 18, pp. 19640-19646, 2021.
- [7] T. N. Pornsin-sirirak, Y. C. Tai, H. Nassef, and C. M. Ho, "Titanium-alloy MEMS wing technology for a micro aerial vehicle application," *Sensors and Actuators A: Physical*, vol. 89, no. 1, pp. 95-103, 2001/03/20/ 2001.
- [8] L. Ednie *et al.*, "The effects of surface finish on the fatigue performance of electron beam melted Ti-6Al-4V," *Materials Science and Engineering: A*, vol. 857, p. 144050, 2022/11/01/ 2022.
- [9] A. D. Di Crescenzo, M. Mousseigne, and W. Rubio, "Effect on surface integrity of high-productivity finishing on Ti-6Al-4V with wiper edge length tool," *Procedia CIRP*, vol. 108, pp. 406-411, 2022/01/01/ 2022.
- [10] N. A. Mutalib, I. Ismail, S. M. Soffie, and S. N. Aqida, "Magnetorheological finishing on metal surface: A review," *IOP Conference Series: Materials Science and Engineering*, vol. 469, no. 1, p. 012092, 2019/01/01 2019.
- [11] W. Wang, S. Ji, and J. Zhao, "Review of magnetorheological finishing on components with complex surfaces," *The International Journal of Advanced Manufacturing Technology*, vol. 131, no. 5, pp. 3165-3191, 2024/03/01 2024.

- [12] A. S. Rajput, M. Das, and S. Kapil, "A comprehensive review of magnetorheological fluid assisted finishing processes," *Machining Science and Technology*, vol. 26, no. 3, pp. 339-376, 2022/05/04 2022.
- [13] Y. Wang, S. Yin, and H. Huang, "Polishing characteristics and mechanism in magnetorheological planarization using a permanent magnetic yoke with translational movement," *Precision Engineering*, vol. 43, pp. 93-104, 2016/01/01/ 2016.
- [14] H. Luo *et al.*, "An atomic-scale and high efficiency finishing method of zirconia ceramics by using magnetorheological finishing," *Applied Surface Science*, vol. 444, pp. 569-577, 2018/06/30/ 2018.
- [15] M. Nie, J. Cao, J. Li, and M. Fu, "Magnet arrangements in a magnetic field generator for magnetorheological finishing," *International Journal of Mechanical Sciences*, vol. 161-162, p. 105018, 2019/10/01/ 2019.
- [16] M. Xie, Z. An, and J. Zhuang, "Design and experimental research of dynamic magnetic field device based on Halbach array in magnetorheological polishing," *The International Journal of Advanced Manufacturing Technology*, vol. 120, 06/01 2022.
- [17] J. Qin, M. Feng, and Q. Cao, "Processing Optimization for Halbach Array Magnetic Field-Assisted Magnetic Abrasive Particles Polishing of Titanium Alloy," *Materials*, vol. 17, no. 13. doi: 10.3390/ma17133213
- [18] K. Nishimura, "The strongest array beyond Halbach array," *Journal of Magnetism and Magnetic Materials*, vol. 580, p. 170933, 2023/08/15/ 2023.
- [19] J. Ye *et al.*, "Concise magnetic force model for Halbach-type magnet arrays and its application in permanent magnetic guideway optimization," *Journal of Magnetism and Magnetic Materials*, vol. 587, p. 171301, 2023/12/01/ 2023.
- [20] Z. Huang, Q. Yan, J. Pan, Z. Chen, and J. Lu, "Dynamic magnetic field magnetorheological finishing with constant load and variable gap," *Precision Engineering*, vol. 86, pp. 388-399, 2024/03/01/ 2024.